Semiannual Technical Report

Growth of Single Crystals and Fabrication of GaN and AlN Wafers

Supported under Grant # N00014-00-1-0192
Office of the Chief of Naval Research
Report for the period 1/1/00-6/30/00

Z. Sitar. R.F. Davis
R. Schlesser, C. Draper, H. Shin
North Carolina State University
Department of Materials Science and Engineering
Box 7919
Raleigh, NC 27695

July, 2000

REPORT DOCUMENTATION PAGE

Form Approved
OMB No. 0704-0188

1. AGENCY USE ONLY *(Leave blank)*	2. REPORT DATE	3. REPORT TYPE AND DATES COVERED
	July, 2000	Semiannual: 1/1/00 - 6/30/00

4. TITLE AND SUBTITLE

Growth of Single Crystals and Fabrication of GaN and AlN Wafers

5. FUNDING NUMBERS

CFDA: 12.300
DUNS: 008963233
PR: 00PR03598-00
Act.:00312--0051
CAGE: 0ECY3
EDI: 7129AB

6. AUTHOR(S)

Z. Sitar, R. F. Davis

7. PERFORMING ORGANIZATION NAME(S) AND ADDRESS(ES)

North Carolina State University
Hillsborough Street
Raleigh, NC 27695

8. PERFORMING ORGANIZATION REPORT NUMBER

N00014-00-1-0192

9. SPONSORING/MONITORING AGENCY NAMES(S) AND ADDRESS(ES)

Sponsoring: ONR, Code 312, 800 N. Quincy, Arlington, VA 22217-5660
Monitoring: Administrative Contracting Officer, Regional Office Atlanta
Atlanta Regional Office
100 Alabama Street, Suite 4R15
Atlanta, GA 30303

10. SPONSORING/MONITORING AGENCY REPORT NUMBER

11. SUPPLEMENTARY NOTES

12a. DISTRIBUTION/AVAILABILITY STATEMENT

Approved for Public Release; Distribution Unlimited

12b. DISTRIBUTION CODE

13. ABSTRACT ***(Maximum 200 words)***

GaN and AlN single crystals were grown from the vapor phase by evaporation of gallium or aluminum metals under an ammonia or nitrogen flow in a high temperature reactor. A growth rate of 500 μm/hr in the c direction was achieved for GaN while the growth rates for AlN were as high as a few millimeters per hour. The crystal size reached 3 mm for GaN and up to 15 mm for AlN. For both materials, the crystal aspect ratio (c/a) could be controlled by temperature and partial pressure of reactants. The resulting crystals were transparent and of excellent crystalline quality, as confirmed by x-ray diffraction, Raman scattering, and transmission electron microscopy studies. Photoluminescence studies on GaN conducted at 77 K showed a sharp emission peak centered at 359 nm. Time dependent photoluminescence measurements revealed optical metastability in bulk GaN.

14. SUBJECT TERMS

GaN, AlN, bulk crystal growth, growth from vapor phase, photoluminescence, optical absorption, Raman, SIMS.

15. NUMBER OF PAGES

30

16. PRICE CODE

17. SECURITY CLASSIFICATION OF REPORT	18. SECURITY CLASSIFICATION OF THIS PAGE	19. SECURITY CLASSIFICATION OF ABSTRACT	20. LIMITATION OF ABSTRACT
UNCLAS	UNCLAS	UNCLAS	SAR

Table of Contents

Growth of AlN bulk crystals by vapor phase transport

Introduction

The following report summarizes recent progress made in growing AlN bulk crystals from the vapor phase; source materials were either Al metal or pre-reacted AlN, evaporated in a quasi-stagnant nitrogen atmosphere. A dedicated growth reactor was designed and assembled in house. Initial tests of the reactor equipment demonstrated that the required, elevated growth temperatures (2000 - 2400°C) could be reached and maintained for prolonged periods of time. A thorough characterization of the reactor temperature profile was carried out and was found to be in agreement with initial model calculations. First growth runs were performed using Al metal and nitrogen gas, and yielded high-quality AlN crystals of up to 1 cm size. A complete study of the relevant growth parameters is currently in progress; initial results on the influence of temperature on crystal size, morphology and quality will be reported below.

Equipment

The growth reactor consists of a vacuum chamber containing a 2.25" diameter reaction tube made of hot-pressed BN. The reaction tube is heated by a cylindrical, resistive graphite heater (6.5" long) capable of heating the reaction zone up to 2400°C (~12 kW electrical power). The heater assembly is encapsulated in a hot-pressed BN cylinder (wall thickness 0.25"). Porous graphite heat insulation separates the heater assembly from the water-cooled walls of the vacuum chamber. A schematic cross-section of the reactor is shown in Fig.1.

A removable bottom flange allows easy access to the reaction tube; loading and unloading of the reaction crucible is performed via this flange, the crucible being inserted into the hot zone of the reaction tube by means of a variable-length BN support rod. The crucible is made of two, 1" diameter BN containers; the bottom part carries the source material (Al or

AlN), while the AlN crystals grow in the (slightly colder) crucible cap. A small hole (1-2 mm diameter) in the crucible equilibrates nitrogen pressure inside the crucible with that of the reaction tube. By varying the vertical position of the crucible relative to the heater location, more or less steep temperature gradients can be achieved between the source material and the cap of the crucible.

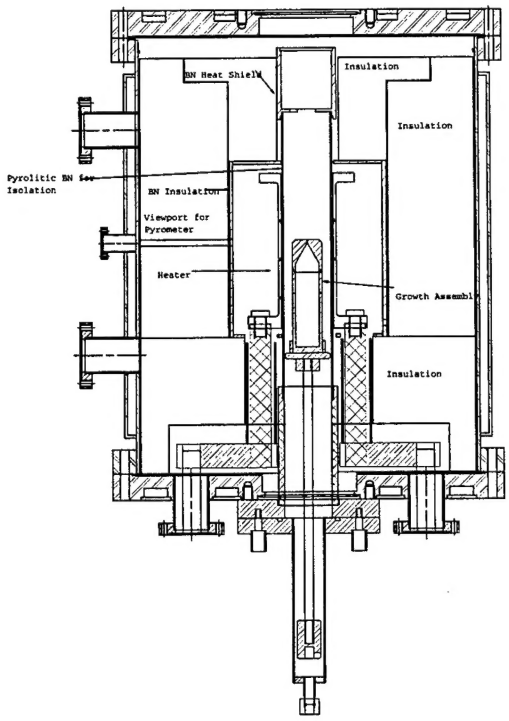

Fig.1 Cross-section of AlN reactor

Due to the elevated temperatures required in the AlN growth process, particular attention was paid to efficient chamber cooling. The chamber body, as well as the bottom and top flanges are double-walled and water-cooled; the electrical feedthroughs carrying current loads of up to 600A are water-cooled as well.

A set of mass-flow controllers allows accurate control of the nitrogen flux (typically 50-100 sccm) into the reaction tube through a bottom-mounted gas inlet. The nitrogen gas flows in an upward motion through the reaction tube, where it passes a set of BN baffles mounted at the top of the tube, before flowing along the inner chamber walls toward a bottom-mounted

pumping port. A rotary pump, in conjunction with an actively controlled butterfly valve provides the required pumping speed to maintain the reactor atmosphere at the desired growth pressure (typically 100-760 Torr).

A small viewport (0.5" window diameter) gives visual access to the heater surface; a single-color pyrometer operating at a wavelength of 2.2μm allows determination of the heater temperature during the growth process. The window is air-cooled by means of a cooling fan in order to keep the temperature of the viewport sufficiently low during operation.

The heater current is provided by two switched power supplies of 375A/40V each, connected in parallel in a master-slave configuration. The reactor equipment is completed by rack-mounted monitoring and controlling hardware. Pressure gauge controllers (1 Baratron, 1 convectron), a butterfly valve controller, mass flow controller electronics, a pyrometer temperature read-out, as well as a Macintosh-based data acquisition system complete the setup. Currently, most growth parameters are adjusted manually by the operator, while the data acquistion system monitors and displays the crucial growth parameters. A safety interlock system is hardwired and monitors cooling water flow, process temperature (high limit), process pressure (high/low limits), as well as heater over-voltage and over-current conditions. Process automation software will be needed to run the equipment over extended periods of time, and is currently under development.

Tests and calibration

Initial tests confirmed that the reactor can be successfully operated at temperatures in the range of 2000-2400°C, and, after minor modifications, chamber cooling was found sufficient for long-term operation of the system. Meanwhile, more than 50 growth runs of 2-4 hours duration have been accomplished; only minor degradation of the graphite insulation has been observed. The initial heater design has been optimized to improve

longevity of the graphite element. Safety interlocks and emergency shutdown procedures were tested.

Temperature profiles of the reaction tube, both longitudinally and laterally, were taken by means of a movable thermocouple. Fig. 2 shows the axial temperature profile, as measured without the crucible installed. As can be seen, depending on the vertical position of the crucible, more or less steep temperature gradients can be achieved, ranging from 0 - 300K/inch.

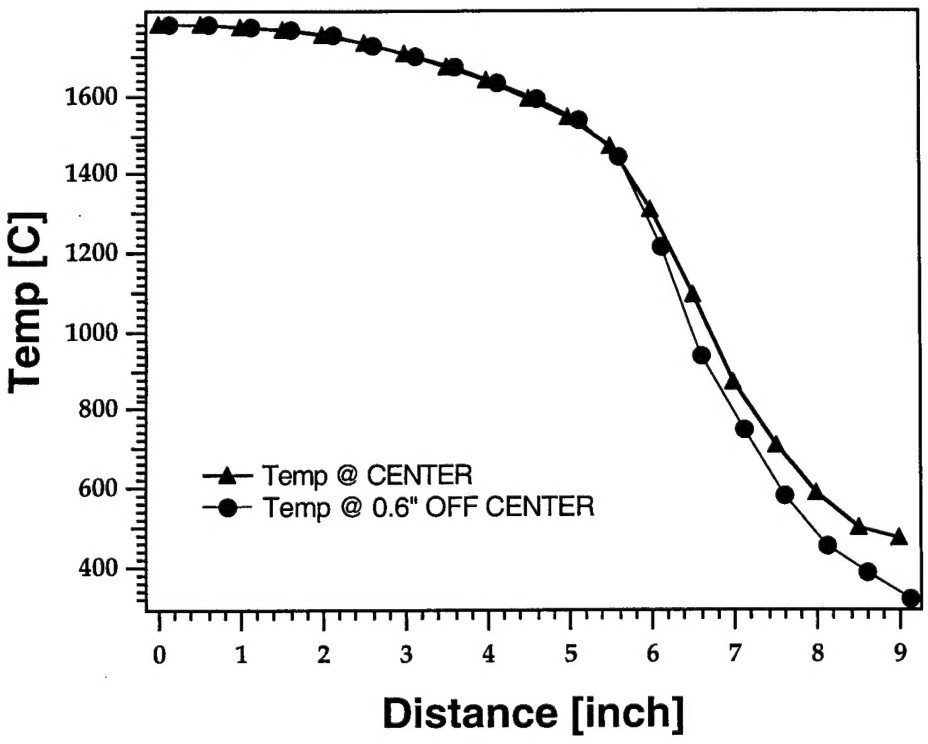

Fig.2 Axial temperature profile of reaction tube.

The pyrometer temperature measurement of the heater surface was carefully calibrated at temperatures in the order of 1000°C by comparison with a thermocouple installed for this purpose only. The transmissivity of the viewport was determined to be 0.90 at a wavelength of 2.2 μm. The apparent emissivity, including the emissivity of the heater surface, as well as the transmissivity losses of the viewport, was found to be 0.86. The uncertainty of

pyrometer measurements was estimated to be ± 50°C (@ 2300°C). The reproducibility from run to run of heater temperature vs. electrical power was excellent within ± 10°C, thus allowing us to control reactor temperature via a feed-forward algorithm utilizing the empirically determined dependence between temperature and power. A feedback algorithm actively regulating heater power as a function of the pyrometer signal was successfully tested, but was eventually abandoned due to safety considerations, as a faulty or misaligned pyrometer would lead to excessive reactor temperatures.

In all experiments the heater surface temperature was used as the main temperature parameter due to the ease of the pyrometer measurement and its excellent reproducibility. The real temperature of the crucible remains unknown, however, the temperature gradient between the heater surface and the center of the reaction tube was determined via a thermocouple measurement to be < 100°C at 1800°C.

Experimental results

After initial test runs, a sequence of growth runs was performed at increasing temperatures. Source material was Al metal, nitrogen flow was kept constant at 50 sccm, and reactor pressure was 500 Torr. AlN crystals were formed by spontaneous nucleation on the crucible walls. As a function of temperature the following results were obtained:

T < 1800°C: only insignificant growth was observed at these temperatures. Reaction between Al and N_2 requires higher temperatures to become efficient.

1800°C < T < 1900°C: AlN needles were grown (see Fig. 3), the long axis of the needles corresponding to the crystallographic c-axis. Estimated growth rates were > 1 mm/hr in c-direction, and 50μm in a-direction.

1900°C < T < 2000°C: twinned a-platelets were formed, some of which grew at rates of several mm/hour.

2000°C < T < 2100°C: c-platelets up to 10x3 mm^2 were grown in 2 hours (see Fig.4). Growth rates up to 5 mm/hr in a-direction, and up to 1 mm in c-direction were observed.

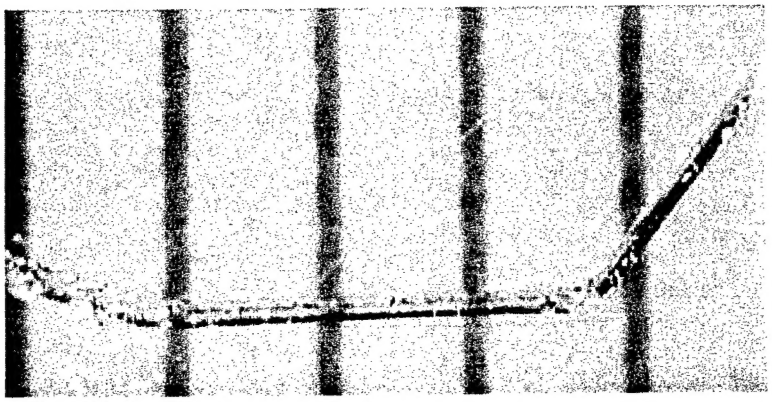

Fig.3 AlN needle grown at 1800°C. Scale markers are separated by 1mm.

Fig. 4 AlN c-platelet grown at 2100°C. Scale markers are separated by 1 mm.

It should be mentioned that these relatively large growth rates observed at temperatures < 2100°C were achieved from Al metal source material. However, as an Al-rich AlN crust typically forms over the Al source during the runs, it is reasonable to assume that the initial growth rate gradually decreased during the runs. Nitrogen flow was 100 sccm, and reactor pressure was 500 Torr. The vertical position of the crucible inside the reaction tube was changed in steps of 0.5" from run to run, and the mass changes of the bottom part of the crucible (source) and the cap (AlN growth) were measured after each run.

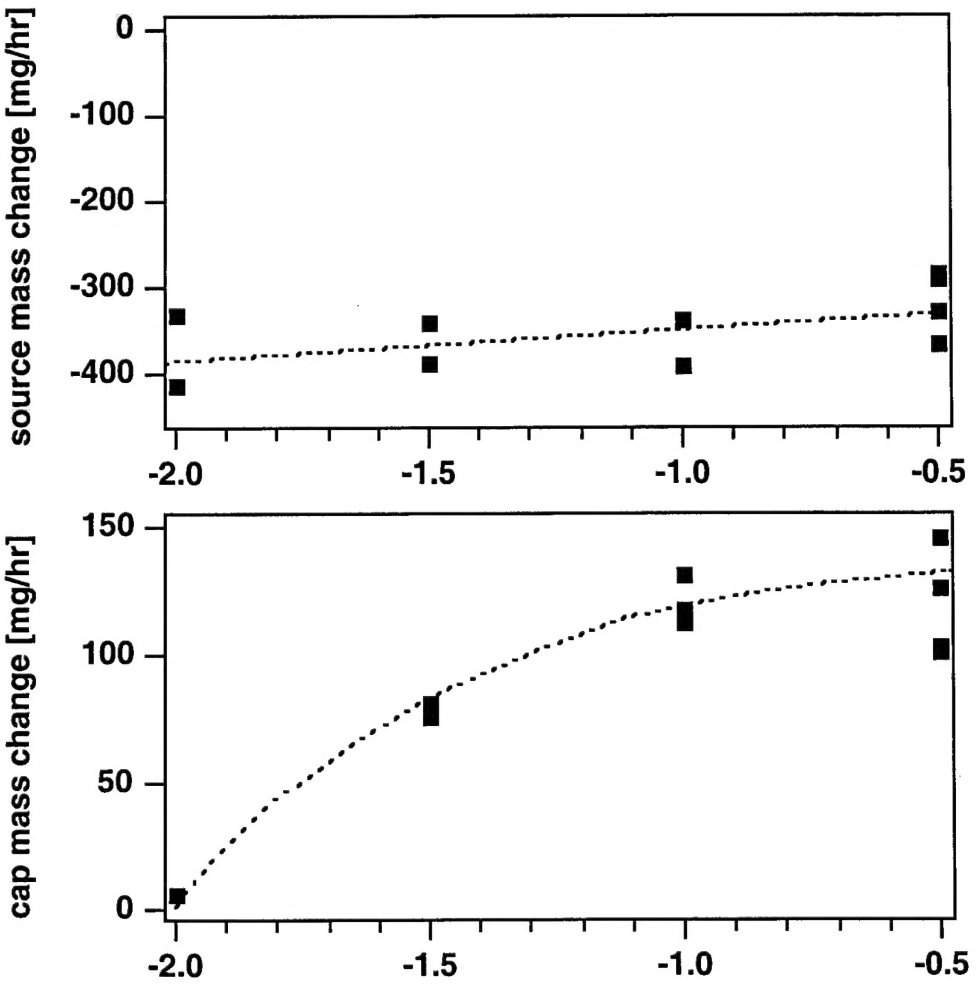

Fig.5 Mass changes of source and crucible cap as a function of crucible position. All other parameters were kept constant. Mass gain in the cap increased as crucible top exited hot zone in the reaction tube, while mass change of source remained virtually constant.

In a second set of experiments, vapor phase transport from an AlN source was investigated as a function of the longitudinal temperature gradient along the crucible. The source material was formed inside the crucible by adding Al metal in several iterations, and subsequently heating the crucible to approximately 1900°C. As AlN source material yields significantly smaller flux of Al than Al metal, this study was performed at higher temperature (2320°C).

Fig. 5 shows that the positive mass change of formed AlN in the crucible cap increases as the gradient between source and cap increases. Mass changes of > 100mg/hr were observed. Mass changes were stable over time and reproducible from run to run.

These experiments yielded valuable information for the planned growth on AlN seeds. We showed that AlN only deposited in the cap area of the crucible, that stable growth rates can be achieved under the above conditions, and we observed that crystals formed in the crucible cap kept growing after having been exposed to air in between runs. All these observations indicate that growth of AlN bulk crystals from seeds should be feasible.

Analytical results

Optical microscopy revealed that the grown crystals were transparent and did not show any coloration, which indicates that the crystals are not contaminated (in particular, carboxy-radicals are known to color AlN crystals blue, while oxygen contamination appears to yield orange coloration).

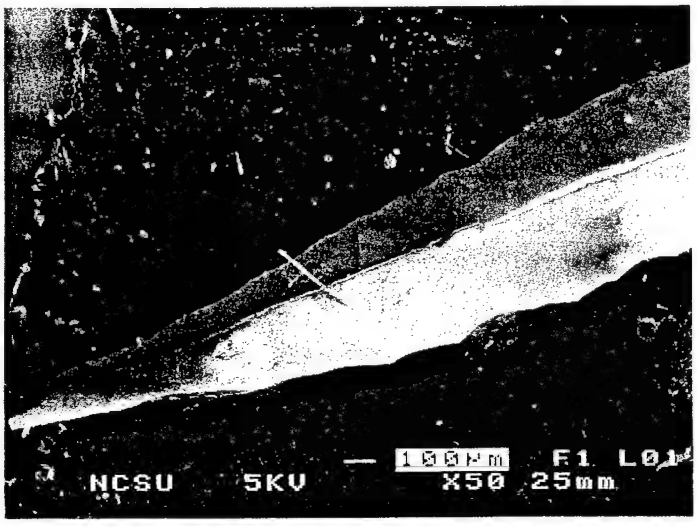

Fig.6 SEM micrograph of a twinned AlN crystal grown at 2000°C.

Scanning electron microscopy (SEM) was employed to observe the surface morphology of the AlN crystals. Fig. 6 shows the surface of a twinned AlN crystal, while Figs. 7 and 8 show c-plates at low and high magnification, respectively.

Fig.7 Low-magnification SEM of a c-plate grown at 2100°C. Hexagonal surface features indicate that the c-direction is normal to the surface.

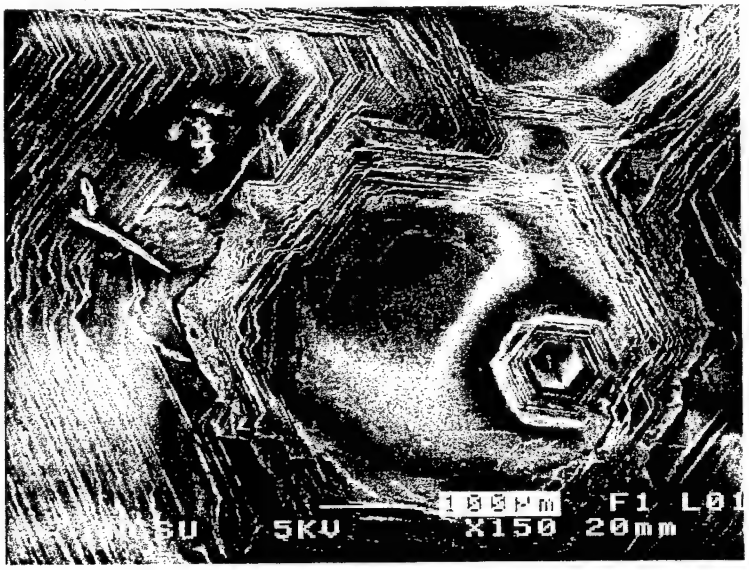

Fig.8 High-magnification SEM of a c-plate grown at 2100°C. The growth on the c-planes occurred by the desired step-flow mechanism.

Raman spectroscopy was employed to further assess the quality of the grown crystals. A sequence of Raman spectra taken from samples grown at 1800°C, 2000°C, and 2100°C shows a drastic improvement in crystal quality with increasing temperature, see Fig. 9.

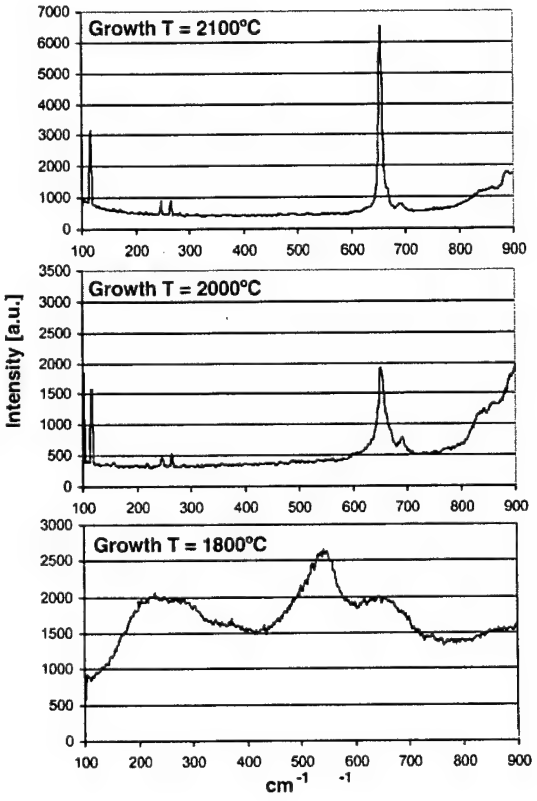

Fig.9 Sequence of Raman spectra documenting increasing crystal quality with growth temperature.

Summary

The AlN growth equipment has been successfully tested and calibrated. First growth runs yielded high-quality AlN crystals of up to 1 cm size. Growth temperature was found to have a crucial effect on crystal morphology and quality. AlN growth from both, Al metal and AlN sources, has been achieved. Vapor phase transport from AlN source material has been investigated quantitatively and crystal weight increases linearly with the growth time. The growth from the Al source occurs at a lower temperature and the growth rate is about one order of magnitude faster than from the AlN source, however, a study of this growth

rate as a function of time has to be performed. Further parametric studies, investigating the influence of reactor pressure and nitrogen flow are under investigation. Growth from AlN seeds will be performed in the near future.

Growth of GaN bulk crystals by vapor phase transport

Abstract

Up to 3 mm long GaN single crystals were grown by sublimation of cold pressed GaN pellets or evaporation of gallium (Ga) metal under an ammonia (NH_3) flow in a dual heater, high-temperature growth system. A growth rate of 500 μm/hr along the [0001] direction was achieved using a source temperature of 1200°C, a total pressure of 760 Torr, and an NH_3 flow rate of 50 sccm. The resulting crystals were transparent, possessed low aspect ratios and well-defined growth facets. The only impurity present at high concentrations was oxygen (3×10^{18} atoms/cm^3). Photoluminescence studies conducted at 77 K showed a sharp emission peak centered at 359 nm. Time dependent photoluminescence measurements revealed optical metastability in bulk GaN. Raman spectroscopy yielded narrow peaks representing only the modes allowed for the wurtzite structure. All characterization studies confirmed excellent crystalline and optical quality of the obtained single crystals.

Introduction

The achievement of blue and green light emitting diodes and blue emitting lasers [1], as well as prototypes of several microelectronic devices produced from GaN-based materials is intriguing, given the high density ($\geq10^9$ cm^{-2}) of dislocations present in most device structures. Substantial defect reduction via the use of lateral overgrowth techniques and substrate removal have resulted in reported lifetime assessments of 10,000 hours for the blue laser diodes [2]. This has had a significant impact on the commercial importance of this material [3]. However, the increased number of process steps leading to defect reduction increases the fabrication costs of devices. The availability of low defect density GaN substrates on which homoepitaxial films can be grown should result in marked improvements in device performance at reduced cost.

Growth of the GaN bulk crystals is a challenge due to its high melting temperature, low sublimation/decomposition temperature relative to its melting temperature, very high equilibrium nitrogen vapor pressure at moderate temperatures, and low solubility in acids, bases and most other inorganic elements and compounds. Novel bulk growth techniques must be employed which either take advantage of these inherent properties or surmount the difficulties presented by them.

Elwell and Elwell [4] reviewed the bulk GaN crystal growth research to 1988. The two most widely investigated approaches to date have been solution growth [5-10] and vapor phase transport [11-15]. The success of these methods has been limited to small crystals. The use of high-pressure solution synthesis has resulted in increasingly larger crystals. The initial research [13,14] with this last technique produced thin platelets limited in size to ≈1 mm. Recent research by these authors has resulted in crystals 8 mm square × 0.2 mm thick grown at a rate along the c-axis of ≈20 μm/hr [10]. As reported, crystal quality decreased with increasing platelet size. Homoepitaxial thin film growth on good sections of these crystals resulted in a marked improvement in defect reduction relative to the films grown on foreign substrates.

Vapor phase transport has been employed by Sakai and co-workers [16] for the growth of GaN needles on sapphire substrates via sublimation of GaN powder in a flow of NH_3. The average crystal size was reported to be a few hundred micrometers. Homoepitaxial film growth by these investigators also resulted in decreased defect densities relative to films grown on foreign substrates. The above results indicated that bulk crystal growth of GaN can be achieved; however, the parameters necessary to enhance the size and quality of the crystals are rather precise and must be closely controlled.

The research described in the following sections deals with GaN crystal growth from the vapor phase via evaporation of Ga metal or sublimation of GaN powder in an NH_3

environment at temperatures higher than reported previously. Comparisons of optical microscopy, photoluminescence (PL), Raman spectroscopy, and secondary ion mass spectroscopy (SIMS) results with those available in the literature indicate that crystals grown in this research by this technique are of excellent quality.

Experimental Procedures

Consolidation of Gallium Nitride Powder. Consolidated GaN powder was selected as one of the source materials for the crystal growth experiments. Compact shapes are easier to contain during sublimation at low pressures and provide flexibility in positioning the source material.

Gallium nitride begins to decompose above 800°C under one atmosphere of nitrogen [17]. The melting point of GaN is not known; however, most theoretical estimates place it above 2000°C. Bulk diffusion, sufficient to achieve densification in refractory materials, is usually achieved at approximately two-thirds of their respective melting points; therefore, densification via sintering was impossible, even with small grain size material. Hot and cold isostatic pressing were deemed the most feasible methods for densification of this material.

Compacting GaN powder via the first method was unsatisfactory. High purity GaN powder produced in our laboratory [18] was successfully compacted into pellets via cold isostatic pressing. This powder possessed exceptional structural quality and has been classified as the new X-ray standard (* quality) for this material [19]. The powder was subsequently jet milled (Model 00 Jet-O-Mizer grinding system at Fluid Energy Aljet Inc, PA) in an N_2 ambient. The feed rate and manifold pressure were 75 grams/hr and 7 kg/cm^2, respectively. Reduced particle size and improved particle uniformity were obtained which enhanced the cold pressing results.

Cylindrical pellets, 13 mm diameter and 6 mm in height, were prepared in stainless steel dies using an uniaxial cold press at pressures between 1575-2200 kg/cm^2. Delamination of the pellets was observed above 1750 kg/cm^2. The pressure range of 1650-1700 kg/cm^2 was optimum. Pellets used for the crystal growth experiments were pressed at 1700 kg/cm^2. Approximate green densities ranged from 60-70% of theoretical. Firing the GaN pellets in N_2 atmosphere at 700°C resulted in a negligible increase in density.

Crystal Growth. Crystal growth of GaN was achieved by subliming cold pressed pellets of GaN in a stream of 99.9999% pure NH_3 gas. An alternative route of crystal synthesis employed the evaporation of 99.999% pure elemental Ga in the same purity of NH_3. All experiments were conducted in a dedicated system, specifically designed for GaN crystal growth. The reaction tube was isolated from the heaters and contained the source and seed materials. Two independently controlled heaters were used to achieve the temperature gradient necessary for growth. The growth system is shown schematically in Figure 1.

The source and seed holder assemblies were manufactured from hot pressed boron nitride (BN) having an open porosity of 9%. The BN was chosen due to its ease of machining and inertness to NH_3. Blank BN seed holders served as the primary nucleation surfaces; however, 6H-SiC (0001) seed crystals were used in a limited number of experiments. A source-to-seed distance of ~25 mm was employed in all experiments. The experimental arrangement allowed NH_3 to flow from the top.

All growth experiments were performed within the range of 1100–1450°C at the source heater and 1200°C at the seed heater. Growth pressures of 50–760 Torr were investigated; however, most experiments were conducted at 600 Torr. An NH_3 flow rate of 50 sccm was used for all experiments.

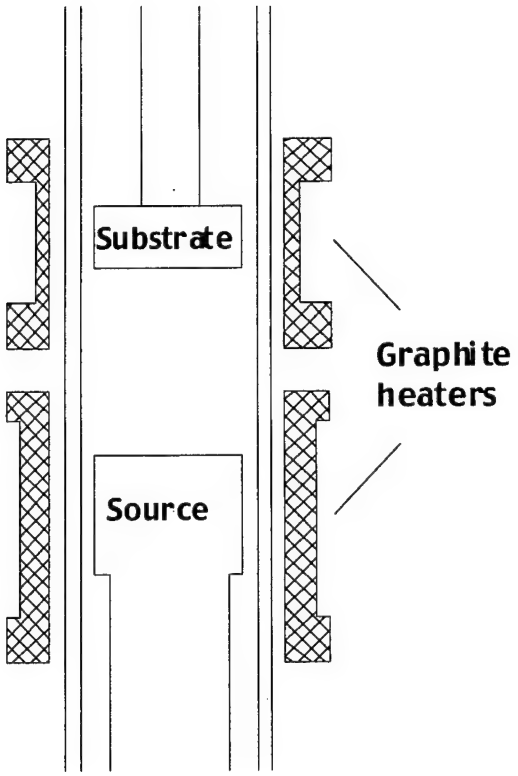

Figure 1. Schematic of the dual heater system used to grow GaN crystals.

Characterization. The presence and concentrations of impurities in the GaN crystals were determined using a Cameca SIMS employing a 10 keV O_2^+ primary ion beam rastered over a 100 μm^2 area. The O_2^+ current was varied from 10 to 100 nA to obtain optimum secondary ion signal levels. The sample was biased at 4500 V, and the presence of H, C, O, Si and Ga (matrix reference signal) was investigated. Impurity concentrations were quantified using standards consisting of the impurity of interest implanted into monocrystalline GaN films grown in this laboratory. Data were acquired from both the standard and the samples under identical instrumental conditions. A relative sensitivity factor (RSF) was then obtained from the standard utilizing a known implanted impurity dose. The sample data were quantified by first taking the ratio of the intensity of the impurity of interest to the matrix reference signal and multiplying the result by the RSF.

Micro-Raman spectra of the GaN crystals were obtained at room temperature using a back scattering geometry from the [0001] face and the 514.5 nm line of an Ar-ion laser. The spot size and the spectral resolution were 4 μm and 2 cm^{-1}, respectively.

The PL studies employed a frequency tripled, mode-locked, femtosecond (fs), titanium:sapphire laser. The duration of the excitation pulses was ≈250 fs. The emitted light was collected, collimated, and focused onto the entrance slits of a 0.32 m spectrometer. The signal was detected using a cooled gallium arsenide array detector. The PL studies were performed on the crystalspressed into indium metal bonded to a copper plug. The samples were oriented with their a-axis perpendicular to the laser beam.

A Cary 5 absorption spectrophotometer was used for the optical absorption studies. An ultraviolet grade optical fiber suitable for the sample size was used to project the light from the monochromator onto the sample. This was necessary, since any light not collected by the detector due to scattering or other phenomena would appear in the data as being absorbed. An S-20 photomultiplier tube (pmt), sensitive to ultraviolet light, was used to collect the light transmitted through the sample. A lock-in amplifier or an electrometer were used to detect the signal. Each scan was baseline corrected. The transmission curves were normalized to 650 nm, where the samples were known to be essentially transparent, and adjusted for the dark current of the pmt above the band gap.

Results and Discussion

Hexagonal single crystals of colorless GaN up to 3 mm in length were grown by spontaneous nucleation on hot pressed BN surfaces from either cold pressed GaN pellets or Ga metal in a stream of ammonia. Figure 2 shows an optical micrograph of ≈1 mm long, well faceted, transparent GaN crystals with low aspect ratios. The shape of these crystals is in great contrast to the needle-shaped crystals grown via vapor phase reaction by other

authors. The growth time, pressure, and temperature of the BN surface used for the growth of these crystals were 2.5 hrs, 600 Torr, and 1000°C, respectively.

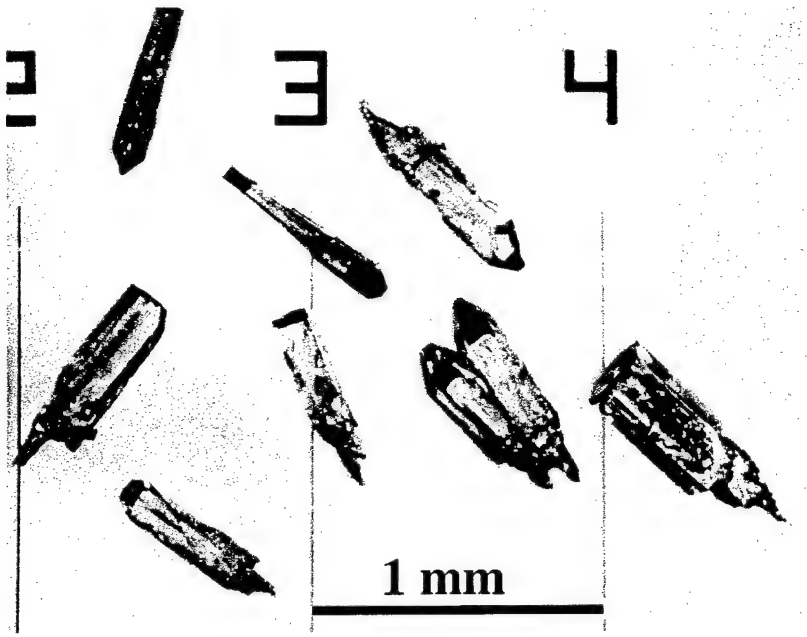

Figure 2. Optical micrograph of selected GaN crystals with low aspect ratios.

The majority of the experiments using the GaN pellets were conducted at a source temperature of 1200°C; above this temperature and under an NH_3 flow rate of 50 sccm, the GaN source began to convert to Ga metal. After each run, the pellets appeared darker in color due to nitrogen loss and small metallic Ga droplets were observed on the surface which became larger (millimeter size) in prolonged runs. Increasing the growth time beyond 2-3 hours yielded GaN crystals that ranged from amber to gray in color, indicative of nonstoichiometric concentrations of nitrogen in the lattice. This is believed to be caused by the combination of a changing crystal surface temperature and an insufficient N incorporation. As the crystals grew, the temperature at the growth surface very likely decreased leading to lesser N incorporation and reduced growth rates. The temperature drift within the growth cavity was probably due to changing surface emissivity as more material was deposited on the inner walls of the crucible. Such changes would effect the kinetics of

the NH_3 decomposition, as well as the source material surface temperature. It is, therefore, essential to control the growth in such a way that it occurs only at one selected growth site.

When metallic gallium was used as a source material, source temperature had to be reduced to prevent oversupply of Ga, since the vapor pressure of Ga over its melt is much higher than that over GaN. In addition, Ga reacts vigorously with ammonia in the temperature range from 950 to 1100°C, resulting in powder formation and coverage of the entire interior of the growth assembly. This reaction can be avoided if the system is held above this temperature range. Due to the above two constraints, the temperature of the Ga source had to be controlled in a relatively narrow range. In these experiments, the temperature was not high enough to prevent the formation of a thin skin of GaN on the surface of the molten Ga. The formation of this layer likely reduced the Ga flux, as increased growth times using metallic Ga as a source did not yield larger crystals. Experiments to establish the conditions under which the thickness of this skin and the supply of Ga can be maintained constant during a run are under way.

The direction of the fastest growth and, thus, the crystal morphology were observed to change with the changing Ga/NH_3 flux ratio and the growth temperature regardless of the Ga source. This was a significant observation in that all previous reports indicated that the growth of bulk GaN from the vapor phase resulted primarily in long needles. The aspect ratio of GaN crystals decreased with increasing Ga/NH_3 ratio. Growth at high Ga/NH_3 ratios resulted in the formation of a mixture of GaN powder and plate-like crystals, which were darker in color in comparison to those grown at a lower Ga/NH_3 ratio. The latter were transparent and needle-like in morphology. It is difficult to assess the independent effect of temperature on crystal morphology in the present system, since the decomposition kinetics of NH_3 changes with temperature. However, it can be stated that the needle-like crystals were grown at a relatively cooler site in the system. Figures 3 and 4 show SEM images of a crystal which grew from a single isolated nucleation site (the bottom right corner of Figure

3) and developed into a well faceted hexagonal shape terminated by flat (10$\bar{1}$ 0) and (0001) planes.

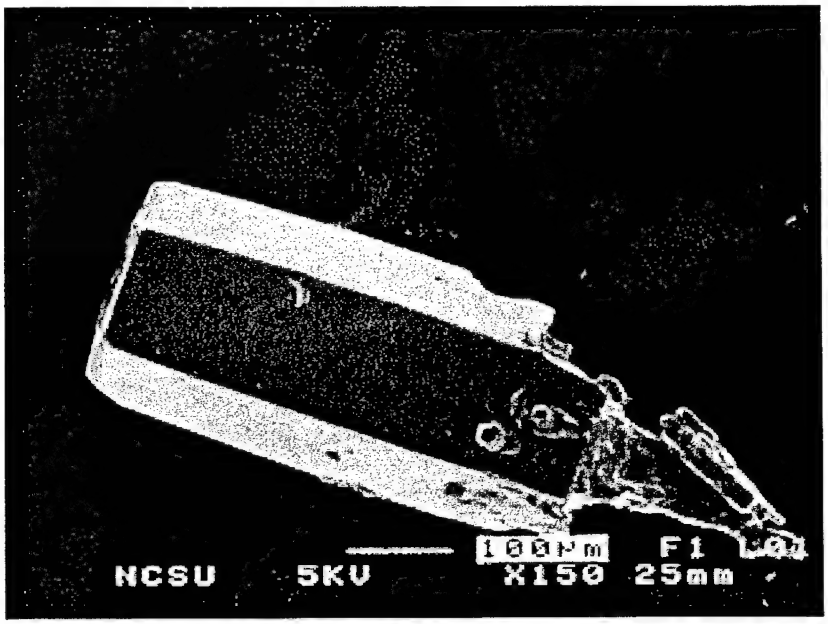

Fig. 3. SEM image of a one mm long GaN crystal with a low aspect ratio showing well developed (10$\bar{1}$ 0) and (0001) crystallographic facets.

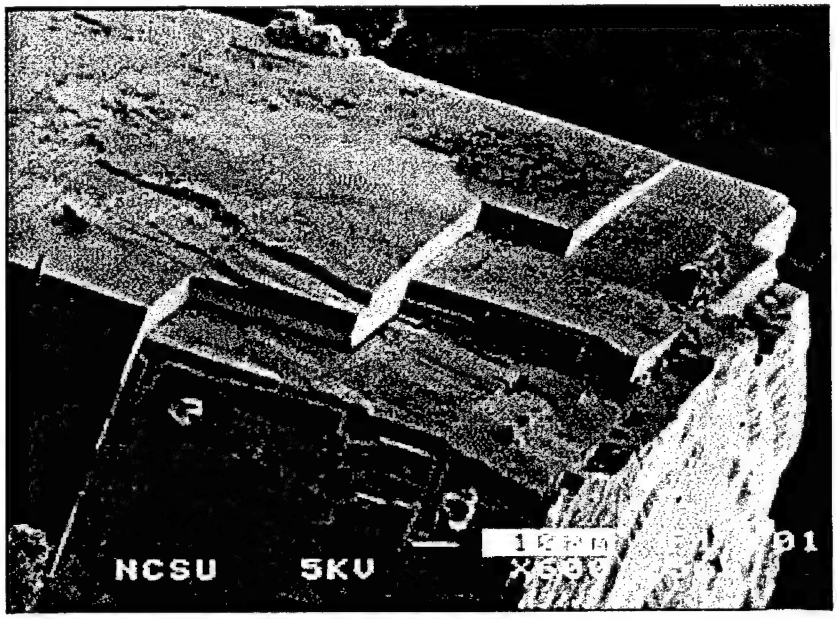

Fig. 4. High magnification of the crystal from Figure 3 showing the growth habits on (0001) and (10$\bar{1}$ 0) planes.

A SIMS scan indicated that all impurities with the exception of oxygen were at background levels. The quantitative results for C, H, O and Si are presented in Table I. These impurity levels are similar to those detected in the CVD grown high-quality GaN thin films [20]. Oxygen incorporation can likely be further minimized by using a higher grade of NH_3.

Table I. Results of the SIMS analysis of the grown GaN crystals

Element	Concentration (atoms/cm^3)
C	2×10^{16}
H	5×10^{16}
Si	1×10^{16}
O	3×10^{18}

A representative PL spectrum for bulk GaN taken at 300 K is shown in Figure 5. Strong bound exciton emission with a peak position at 365.0 nm (3.4 eV) and a FWHM of 9.0 nm (83 meV) was observed. The visible portion of the PL spectrum is expanded 500 times in the inset in Figure 5. No yellow luminescence was detected. The spectrum obtained at 77 K had a peak positioned at 359.0 nm with a FWHM of 54 meV. A slight red shift, as compared to the results from the GaN thin films, is believed to arise due to the lack of stress in bulk crystals.

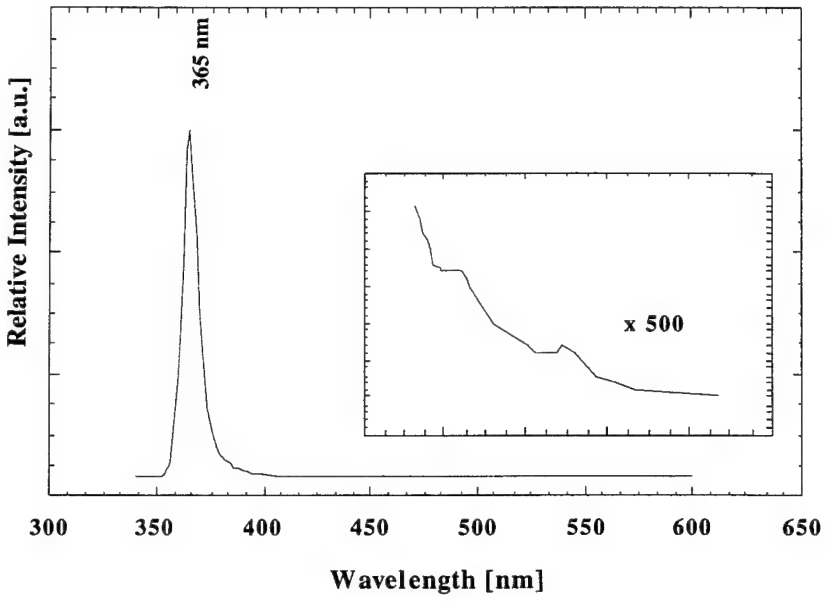

Fig. 5. Photoluminescence spectrum of bulk GaN taken at 300 K. Spectrum lacks yellow luminescence characteristic of defective GaN.

Data representative of the time-dependent photoluminescence obtained at 77 K in five minute intervals are shown in Figures 6 (a)-(d). The first emission spectrum (Figure 6 (a)) corresponds to the band edge emission (peak wavelength = 359 nm, FWHM = 54 meV). After some time, a new emission band started emerging on the long wavelength shoulder of the original luminescence peak and the luminescence changed from invisible to blue. After the sample had been exposed to the pump-light for 22 minutes (spectrum 6 d), the photo induced emission band was centered at 388 nm and included LO-phonon replicas with zero-phonon peak centered at 378 nm. The energy separation between the phonon peaks was about 85 meV, which is close to the reported value of 90 meV for the LO-phonons in wGaN [21]. The FWHM of the blue emission was 249 meV. The significant spectral width of the phonon-assisted recombination implies a strong lattice interaction.

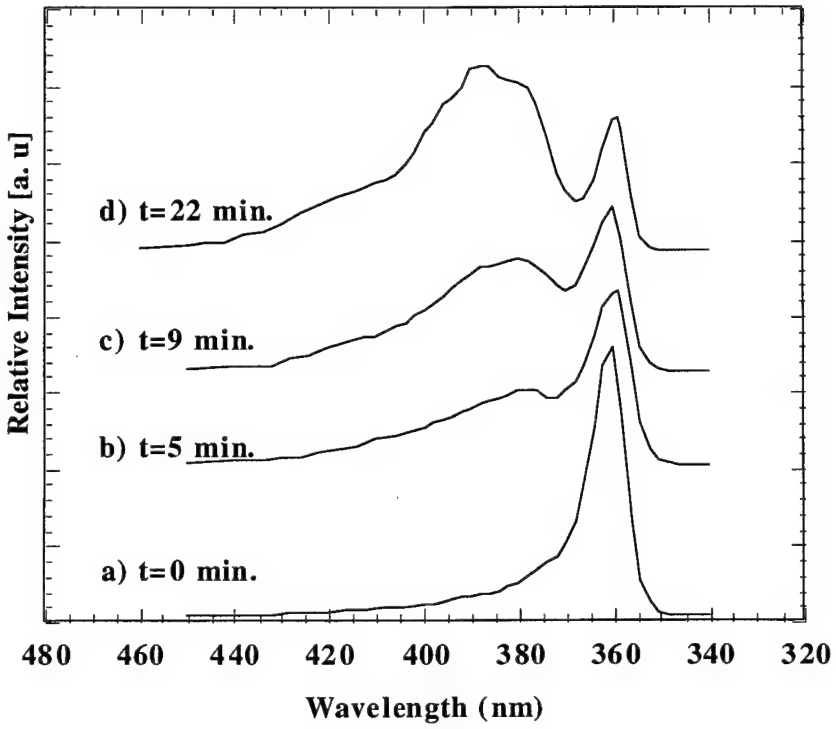

Fig. 6. Time dependent photoluminescence spectrum of bulk an taken at 77 K. The low energy peak became progressively more intense with the illumination time.

A Raman spectrum acquired in a back scattering geometry from one of the grown GaN crystals is presented in Figure 7. The spectrum exhibits only the allowed modes; this implies that the material lacks significant concentrations of structural defects or internal stress, which are known to relax the selection rules. The conservation of the selection rules is indicative of excellent crystallinity. The inset in this Figure shows that the $E_2^{(2)}$ mode is at 567 cm^{-1} and has a FWHM of 3.5 cm^{-1}. These values are indicative of a material of the highest quality reported to date [22].

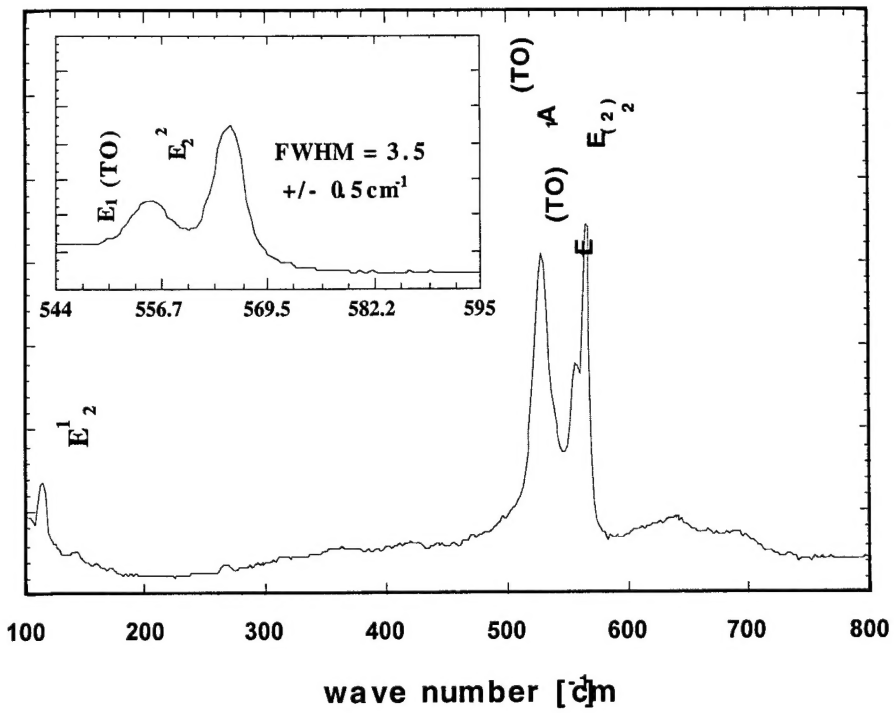

Fig. 7. Raman spectrum of GaN; present are only the allowed Raman modes.

The results of the optical absorption study performed on a 300 μm thick crystal at room temperature are shown in Figure 8. The absorption edge was positioned at 369 nm and was about 10 nm wide. The absorption coefficient over the wavelength range from 400 to 650 nm was estimated to be 50 cm^{-1}. A low absorption coefficient and a narrow absorption edge imply that the bulk GaN crystals are also of high optical quality. The slope in the visible part of the spectrum probably arose due to scattering on the unpolished crystal surface.

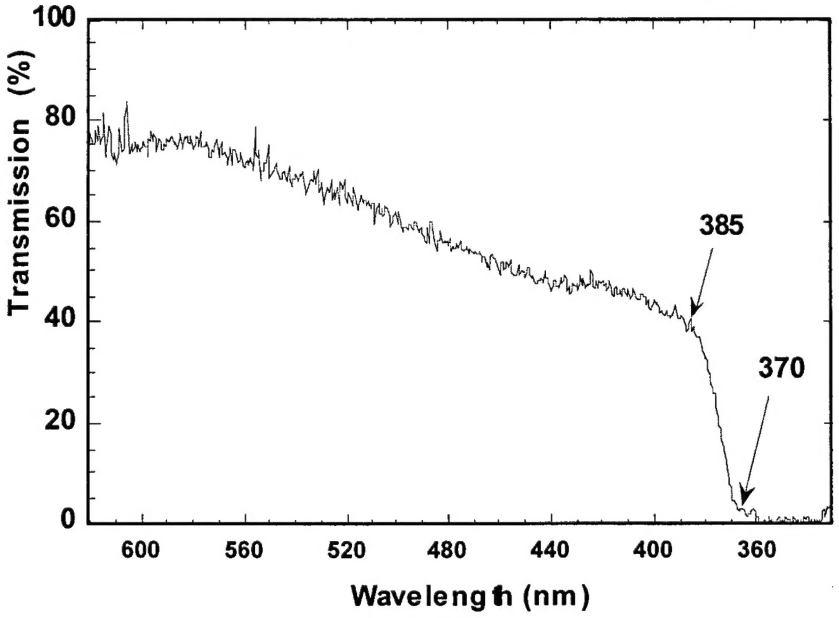

Fig. 8. Optical absorption spectrum of GaN. The absorption edge is at 369 nm and is about 10 nm wide.

Summary

Growth of up to 3 mm long bulk GaN crystals was achieved via sublimation of cold pressed GaN pellets or evaporation of Ga metal in flowing NH_3. The experiments were conducted at a growth temperature, pressure, and NH_3 flow rate of 1000°C, 600 Torr and 50 sccm, respectively. The concentrations of all impurities but oxygen were below the detection limits of SIMS ($\leq 10^{16}$ atoms/cm^3); the concentration of oxygen was measured to be 3×10^{18} atoms/cm^3. Sharp bound exciton emission was observed in the PL spectra of these crystals; no yellow luminescence was observed. An optical absorption edge of 369 nm and an absorption coefficient in the visible spectrum of 50 cm^{-1} were determined. The Raman spectrum was in a complete agreement with the selection rules for the wurtzite structure and showed narrow and well positioned peaks with the $E_2^{(2)}$ mode at 567 cm^{-1}. All these results

References

1. S. Nakamura, M. Senoh, N. Iwasa, S. Nagahama, Jpn. J. Appl. Phys. 34, L797 (1995).
2. S. Nakamura, M. Senoh, S. Nagahama, N. Iwasa, T. Yamada, T. Matsushita, H. Kiyoku, Y. Sugimoto, T. Kozaki, H. Umemoto, M. Sano and K. Chocho Appl. Phys. Lett. 72, 211 (1998).
3. M. Meyer, Compound Semicond. 3, 8 (1997).
4. D. Elwell and M. M. Elwell Prog. Crystal Growth and Charact. 17, 53 (1988).
5. C. J. Frosh, J. Phys. Chem. 66, 877 (1962).
6. R. A. Logan and C. D. Thurmond, J. Electrochem. Soc. 119, 1727 (1972).
7. T. Ogino and M. Aoki, Oyo Butsuri 48, 269 (1962).
8. J. Karpinski, J. Jun and S. Porowski, J. Cryst. Growth 66, 11 (1984).
9. J. Karpinski, and S. Porowski, J. Cryst. Growth 66, 1 (1984).
10. S. Porowski, J. Cryst. Growth 166, 583 (1996).
11. E. Ejder, J. Cryst. Growth 22, 44 (1974).
12. M. Gershenzon, ONR Rept. 243-004F, May (1981).
13. I. G. Pichugin and D. A. Yaskov, Neorg. Mat. 6, 1973 (1970).
14. D. Elwell, R. S. Feigelson, M. M. Simkins and W. A. Tiller, J. Cryst. Growth 66, 45 (1984).
15. R. B. Zetterstrom, J. Mater. Sci. Letter 5, 1102 (1970).
16. S. Sakai, S. Kurai, T. Abe and Y. Naoi, Jpn. J. Apl. Phys. 35, L77 (1996).
17. W. Johnson, J. Parsons and M. Crew J. Phys. Chem. 36, 2651 (1932).
18. C. M. Balkaş and R. F. Davis, J. Am. Ceram. Soc. 79, 2309 (1996).
19. C. M. Balkaş C. Başçeri and R. F. Davis, J. Powder Diffraction 10, 266 (1995).
20. M. D. Bremser, Ph.D. Dissertation Thesis, NCSU, Raleigh, NC, USA (1997).
21. R. Dingle and M. Ilegems, Solid State Commun. **9**, 175 (1971).
22. L. Bergman and R. J. Nemanich, Annu. Rev. Mater. Sci. 26, 551 (1996).

Distribution List

Dr. Colin Wood Office of Naval Research Electronics Division, Code: 312 Ballston Tower One 800 N. Quincy Street Arlington, VA 22217-5660	3
Administrative Contracting Officer Office of Naval Research Regional Office Atlanta 100 Alabama Street, Suite 4R15 Atlanta, GA 30303	1
Director, Naval Research Laboratory ATTN: Code 2627 Washington, DC 20375	1
Defense Technical Information Center 8725 John J. Kingman Road, Suite 0944 Ft. Belvoir, VA 22060-6218	2